



DISSOLUTION OF BENZENE IN THE SATURATED POROUS MEDIA

By

Prof. Dr. Abbas H. Sulaymon

Environmental Engineering Department /College of Engineering/University of Baghdad.

Dr. Hatem Asal Gzar

Environmental Engineering Department /College of Engineering/University of Baghdad.

ABSTRACT:

The aim of the present research is to study the dissolution and transport process of benzene as a light nonaqueous phase liquid (LNAPL) in saturated porous media. Unidirectional flow at water velocities ranged from 0.90 to 3.60 cm/hr was adopted to study this process in a three dimensional saturated sand tank (100 cm×40 cm×35 cm). This tank represents a laboratory-scale aquifer. The aquifer was constructed by packing homogeneous sand in the rectangular tank. The experimental results were used to characterize the dissolution behavior of an entrapped nonaqueous phase benzene source in a three dimensional aquifer model. The time invariant average mass transfer coefficient was determined at each interstitial velocity, the values of this coefficient were ranged from 0.016 to 0.061 cm/hr. It was increased proportionally with velocity toward a limiting value. The results show that the concentration of the LNAPL reduces as the distance increased in *x* and/or *z* direction from the source of pollution. In most cases the benzene concentration declines with velocity more than 2.34 cm/hr at downstream of the LNAPL pool.

:

Light nonaqueous phase liquid (LNAPL)

/ 3.60 0.90

.(35 × 40 × 100)

0.016

/ 0.061

/ 2.34

Key words: Light nonaqueous phase liquid, saturated porous media, dissolution, transport, contamination.

1. INTRODUCTION:

The contamination of soil and ground-water by petroleum hydrocarbons has been of major concern over the last two decades. The most frequent cause of contamination is leakage from underground storage tanks, pipelines, spillages from overfilling or accidents during transferring fuel (Moore et al., 1992). When pollution occurs, a number of dangerous substances may migrate through ground-water, enter into the food and water chain, and finally directly or indirectly harm man (Hiscock, 1995; Makri et al., 2006).

Nonaqueous phase liquids are hydrocarbons that exist as a separate, immiscible phase when in contact with water and/or air. Difference in the physical and chemical properties of water and nonaqueous phase liquid (NAPL) resulted in the formation of a physical interface between the liquids which prevents the two fluids from mixing. Nonaqueous phase liquids are typically classified as either light nonaqueous phase liquids (LNAPLs) which have densities less than that of water, or dense nonaqueous phase liquids (DNAPLs) which have densities greater than that of water. The most common LNAPLs related ground-water contamination problems result from the release of petroleum products. These products are typically multicomponent organic mixture composed of chemicals with varying degrees of water solubility. Examples of LNAPLs include gasoline, jet fuel and heating oils. Gasoline is made up of mono-aromatic compounds such as benzene, toluene, ethylbenzene, and xylenes (including ortho-xylenes, meta-xylenes, and para-xylenes), which are collectively called BTEX compounds. These compounds make up about 18 % by weight of gasoline. The effective solubilities of BTEX compounds are lower than their single - compound aqueous solubilities. BTEX represent potential long-term sources for continued

ground-water contamination at many sites (Newell et al, 1995; Phopfi, 2004).

When the BTEX compounds enter the water or food chain, this can be fatal for human life, causing harm in the short or long term. However, benzene is considered as carcinogenic and mutagenic as well as a priority pollutants according to the Environmental Protection Agency (EPA) and National Primary Drinking Standards (Christensen and Elton, 2005 ; Makri et al., 2006).

A NAPL in physical contact with ground-water will dissolve (solubilize, partition) into the aqueous phase. The solubility of an organic compound is the equilibrium concentration of the compound in water at a specified temperature and pressure. For all practical purposes, the solubility represents the maximum concentration of that compound in water (Newell et al, 1995).

The aqueous-phase concentrations of dissolved NAPLs in ground-water are primarily governed by interphase mass transfer processes that often are slow and rate-limited (Mackay et al. 1985).

Only a limited number of experimental studies have focused on characterizing the NAPL dissolution process under three-dimensional flow conditions (Clement et al. 2004; Lee and Chrysikopoulos 2006).

The objective of the present study is study the dissolution of benzene as a LNAPL in three dimensional homogeneous, isotropic, and saturated porous media.

2. EXPERIMENTAL DESIGN:

2.1. Design of the Experimental Aquifer:

The dissolution experiments were conducted in a three dimensional intermediate-scale sand tank model. The



tank was made of 1 cm thick Perspex plates with dimensions of 100 cm long by 40 cm wide by 35 cm high. Two perforated Perspex plates were used, each one located 10 cm away from both sides dividing the tank into three chambers. The middle chamber was filled with saturated porous sand, and the chambers at both sides were filled with water to maintain constant heads. A filtration cloth was fixed on the perforated plates to prevent passing the sand into the chambers at both sides of the aquifer. Figure (1) shows a schematic diagram of the laboratory-scale aquifer and the other auxiliary equipments. The auxiliary equipments consists of a 125 liter storage tank contains tap water, two constant head reservoirs of 20 liter and 3 liter volumes, respectively, and a flowmeter (Cole-Parmer Instrument Co.; Chicago, Illinois 60648).

2.2. LNAPL Pool Formation and Aquifer Packing:

A circular plastic bowl of 15 cm inner diameter and 5 cm height was used to confine the LNAPL (benzene) pool at the surface of the experimental aquifer. The aquifer tank was filled with sand to a height 23 cm, the water cover all the sand. The bowl was inversely placed on the upper surface of the water-saturated sand, so the open side of the bowl directly faced

the sand. The aim of this configuration is to keep the pool within 15 cm of the porous media. The bowl fixed by four screws with the Perspex cover of tank (figure 1). The LNAPL was dyed with Sudan III which is a powdered, nonvolatile organic dye of red color, soluble in hydrocarbons and insoluble in water. The addition of the red dye is to assist in the visual observation of the LNAPL pool. The thickness of the floating LNAPL pool in the bowl is 1 cm. The pool is injected at a rate of 18 ml/hr.

Karbalaa's sand was used as a porous medium. The 1 mm sand was packed into the tank to height 23 cm. This configuration resulted in a packed volume of about $92,000 \text{ cm}^3$ ($100 \times 40 \times 23 \text{ cm}$). The tank was then filled with water (several cm above the upper level of sand) and left overnight to settle and saturate the sand. The system was then flushed at maximum velocity until the effluent water was free of suspended fine material. After ending each experiment, the used sand removed from the tank. The tank was washed and cleaned very well and then fills with new sand in order to be ready for a new experiment. A small stream of 200 mg/l sodium azide solution was introduced to the influent water at the chamber in the left side of aquifer to inhibit biological growth.

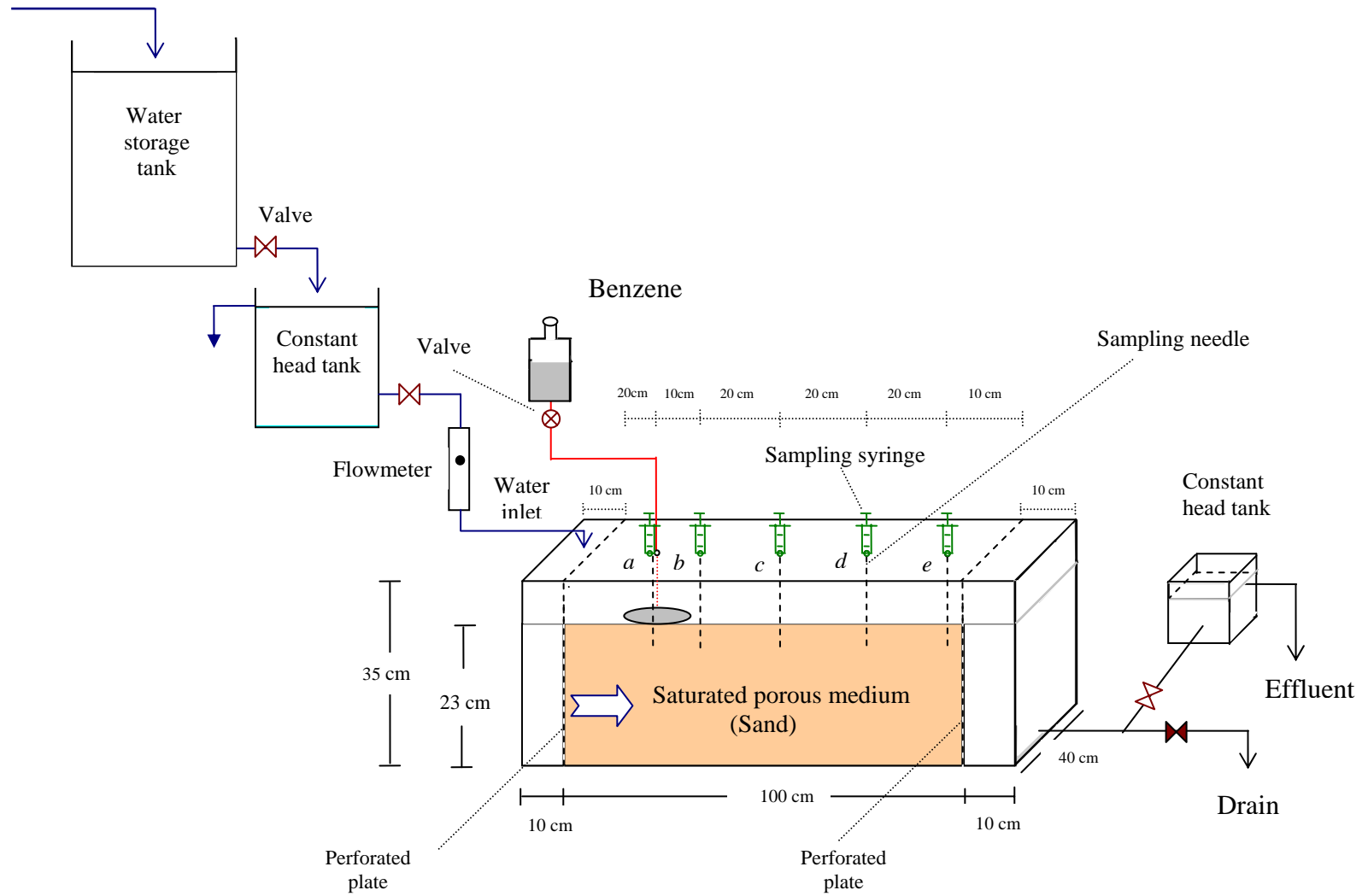


Figure 1: A schematic diagram of the laboratory-scale aquifer (three dimensional sand tank 100×40×35 cm).

2.3. Porous Medium Properties:

Karbala's sand (this type of the soil was taken from the land of Karbala's Governorate in Iraq) was used in the present study as a porous medium. The sand passing through 1 mm mesh was used. Samples were tested for measurement of particle size distribution by mechanical sieve analysis, porosity, as well as the permeability coefficient. All these measurements were achieved at the Soil Laboratory in Civil Engineering Department/College of Engineering/University of Baghdad.

2.3.1. Particle Size Distribution:

The particle size distribution was obtained by using mechanical sieve analysis as shown in figure (2). The uniformity coefficient (C_u), gives an indication of the range of grain sizes presented in a given soil sample (Bowels, 1978; Al-Khafaji and Andersland, 1992). This coefficient was found to be 2.22. The bulk density of the dry sand is 1.6 g/cm^3 , and the porosity is 0.345.

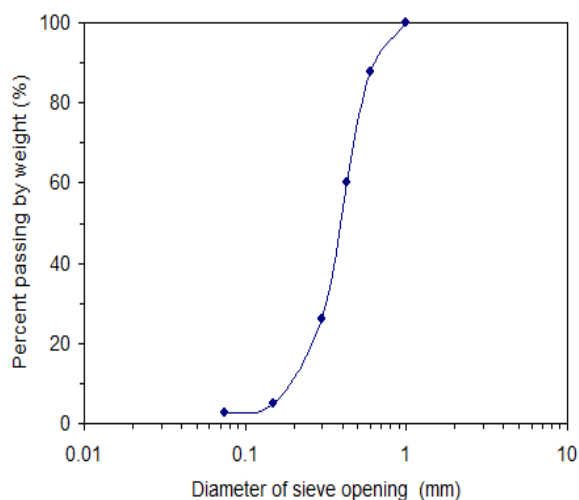


Figure 2: Particle size distribution curve for the Karbala's sand.

2.3.2. Interstitial Velocity:

The Interstitial velocity within the model aquifer was determined by using the

following equation (Chrysikopoulos et al, 2000):

$$V_x = \frac{Q}{wn} \quad (1)$$

where Q is the water volumetric flowrate, w is the aquifer width, h is the head of water in the aquifer, and n is the porosity of porous medium. Five interstitial velocities 0.90, 1.80, 2.34, 2.70, and 3.60 cm/hr were used in the present study.

2.4. Dissolution Experiments:

Five sampling ports (a to e) were conducted on the cover of sand tank. For collecting samples a 15-gauged stainless-steel needles (manufactured by Sherwood Medical St. Louis, Mo, 63103 USA) were inserted into the ports and pushed into the porous medium. Wire inserted inside the needle during the placement process prevented clogging.

Ten dissolution experiments were conducted in the three dimensional bench scale aquifer. These experiments divided into two sets of samples; each one was collected from five selected points within the aquifer downstream from the LNAPL pool at a selected interstitial velocity. The first set was at depth $z = 1 \text{ cm}$, the sampling points located at $(-7.5, 20, 1)$, $(2.5, 20, 1)$, $(22.5, 20, 1)$, $(42.5, 20, 1)$, and $(62.5, 20, 1)$ respectively. The second set of the samples were at depth $z = 3 \text{ cm}$, the sampling points located at $(-7.5, 20, 3)$, $(2.5, 20, 3)$, $(22.5, 20, 3)$, $(42.5, 20, 3)$, and $(62.5, 20, 3)$ respectively. The sampling point $(-7.5, 20, 1)$ and $(-7.5, 20, 3)$ refers to the sampling point below the LNAPL pool at depth 1 cm and 3 cm respectively.

The flow of water from the storage tank and the constant head tank was by gravity. A flowmeter was used to measure the water flow from the constant head tank to the aquifer. For all experiments the

flowrate was ranging from 5 to 20 ml/min. These flowrates yields an interstitial velocity range of 0.90 to 3.60 cm/hr. All experiments were conducted at temperature of $20 \pm 1^\circ\text{C}$. The water elevation in the aquifer was maintained at the desired level by using two constant head reservoirs one before the inlet and the other after the outlet of the aquifer.

2.5. Sample Collection and Analysis:

Aqueous phase LNAPL concentrations were collected only when steady-state concentrations were observed at sampling port (*e*), which is the sampling port farthest away from the LNAPL pool. Interstitial water samples were collected from ports of the sand tank using

needles (figure 1). The volume of syringe used was 5 ml. 1 ml of sample was withdrawn from each location and stored in a glass vial, sealed with teflon-lined septa. The number of collected samples from the five ports in the porous medium was 200 samples at depth 1 cm and 200 samples were at depth 3 cm from the top (figure 3). The samples were analyzed in the Center of Chemical Research and Petrochemical industries/Ministry of the Science and Technology, using Gas Chromatograph equipped with flame ionization detector (Gas Chromatograph GC-2014, Shimadzu Corporation, Analytical & Measuring Instrument Division, KYOTO, Japan).

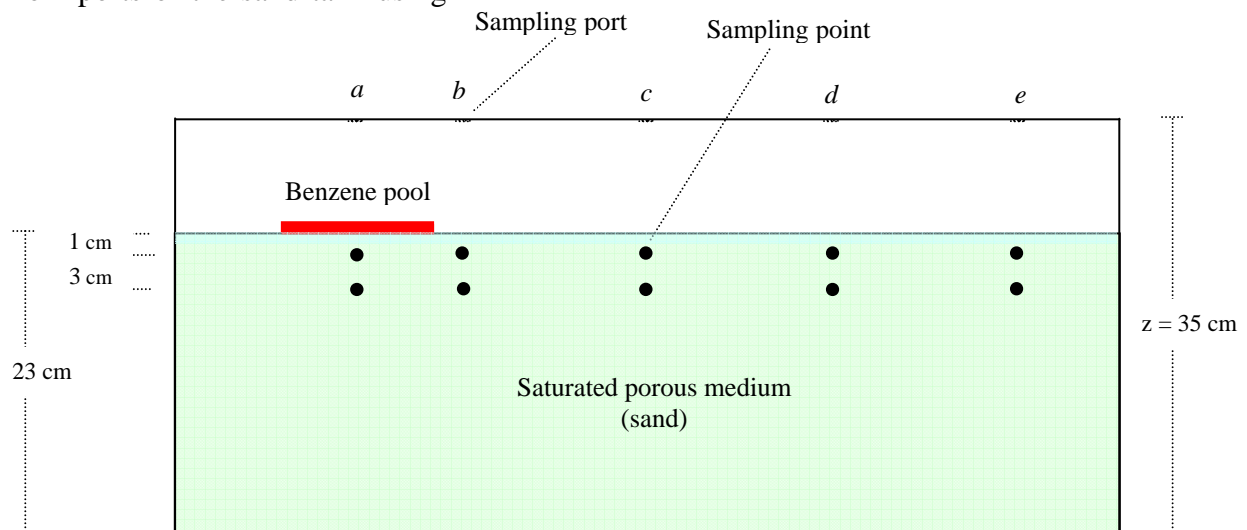


Figure 3: Sketch illustrate *side view* of the model aquifer sampling points location, the points located at depths (*z*) of 1 cm and 3 cm.

3. RESULTS AND DISCUSSION:

Figures (4) and (5) show the change of the measured benzene concentration with distance (*x*) below and downstream of the benzene pool at sampling times of 1, 4, and 8 day. The lateral distance $y = 20$ cm, and at depths (*z*) 1cm and 3 cm, respectively. In general the concentration values decreased with distance. In figure (4), at time 1 day and velocities approximately equal or less than 2.7 cm/hr, the concentrations were increased within the distance -7.5 cm (below the center of benzene pool) to 2.5 cm and then declined to the lower limits, while other profiles have the same

behavior which are decreased with distance from upper to lower limits. In figure (5) which show the concentration versus distance at depth 3 cm, all concentration profiles declined with distance from upper to lower values; except at velocity 3.60 cm/hr; the concentration profile of time 8 day increased within the distance -7.5 cm to 2.5 cm and then continue to decline to the lower limit.

In figure (4), approximately there is no significant difference between the concentration values at time 1, 4, and 8 day with horizontal distance (*x*) except those at the distance between -7.5 cm and



2.5 cm. While in figure (5), a significant difference in concentration was noticed especially at the horizontal distance equal or less than 22.5 cm. The interpreting of this phenomenon may be attributed to effect of many parameters which are collectively effect on the on dispersion and transport of contaminant, these parameters are hydrodynamic conditions such as interstitial velocity (V_x) and dispersion coefficients, and horizontal and vertical (depth) distances.

The effect of the interstitial water velocity on benzene concentration is shown in figures (6) and (7). In these figures; except at distance -7.5 cm, and at distance 2.5 cm in figure (7); the measured concentrations declined at velocities more than about 2.34 cm/hr. The interpretation for this behavior is the increasing of interstitial velocity led to increasing the value of horizontal advection which means that the amount of concentration downstream will be reduced. At the distances -7.5 cm and 2.5 cm where the sampling points situated in holes *a* and *b* ;under and near the benzene pool (at $x = -7.5$ cm, $y = 20$ cm, $z = 1$ cm; $x = -7.5$ cm, $y = 20$ cm, $z = 3$ cm; and $x = 2.5$ cm, $y = 20$ cm, $z = 3$ cm); the behavior of concentration was differ than that of the other figures. In figure (6) at distance -7.5 cm where the sampling point located at the center line below the benzene pool, for the times 1

day and 4 day the concentration increased with increasing velocity; while at the time of the 8 day, the concentration decreased until the velocity reach about 2.34 cm/hr then it is increased with increasing the velocity. In figure (7) at distance -7.5 cm, the concentrations at time 1 day were increased with increasing velocity but then decreased after velocity of 2.34 cm/hr. At times 4 day and 8 day in this figure, and at all times at distance 2.5 cm, the concentration profiles are fluctuated and unstable with increasing velocity.

Clement et.al. (2004) reported that at high velocity, the net flow through the system will increase and therefore the overall dispersion and dilution rates would have also increased; this should have had a negative influence on the downstream concentration levels. On the other hand, the high velocity conditions would have increased the overall dissolution rate because of the presence of high concentration gradient and better mixing conditions near the LNAPL-water boundary; this should have had a positive influence on the downstream concentration levels. Further, high velocities might have also influenced the time-dependent variations in the morphology of the LNAPL source. It is difficult to conceptualize the combined influence of all these complex processes that have offsetting effects.

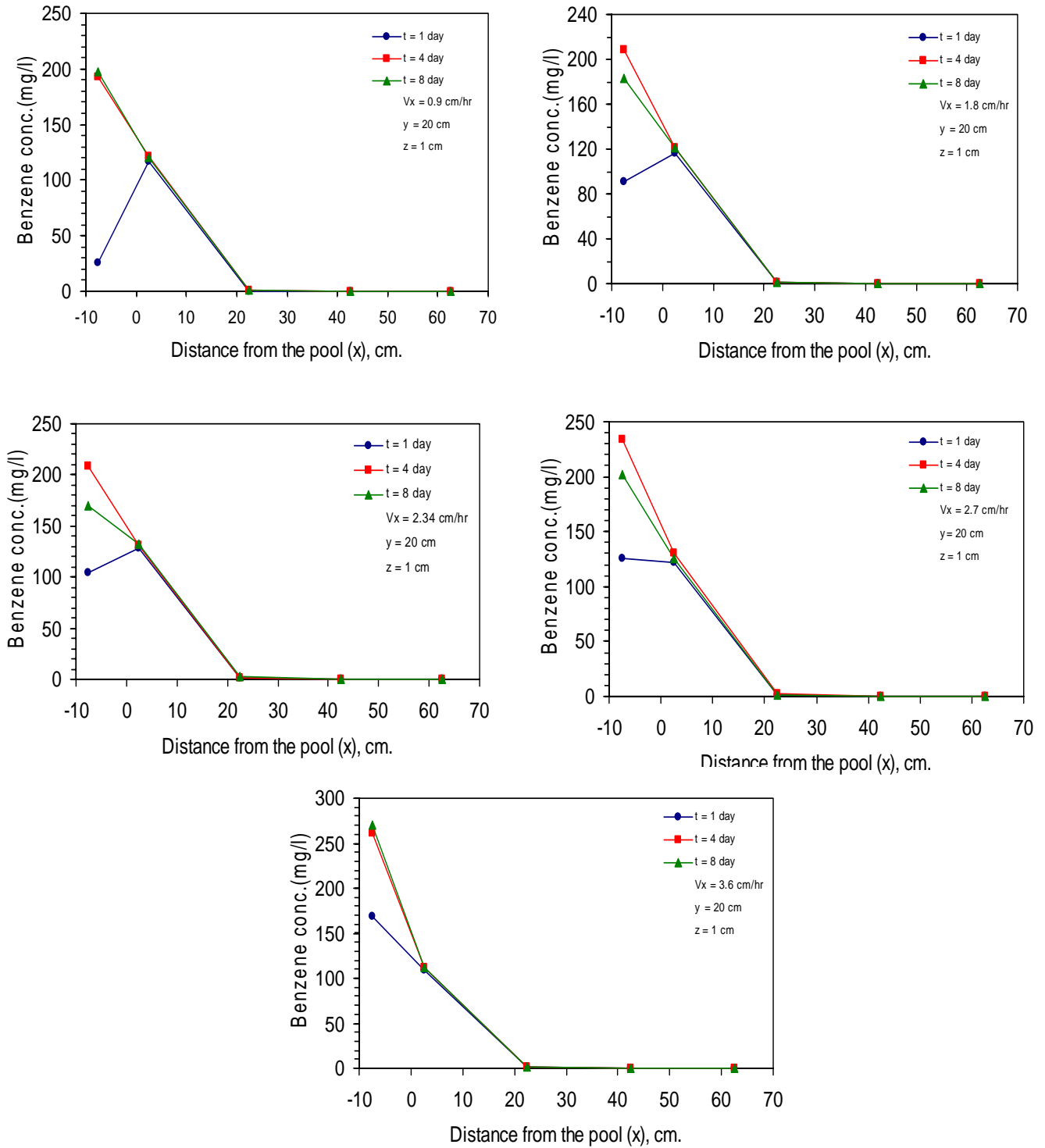


Figure 4: The measured concentration of benzene versus distance from the pool (x) at interstitial velocity 0.90, 1.80, 2.34, 2.70, and 3.60 cm/hr, depth (z) = 1 cm, $y = 20$ cm, and times 1, 4, 8 day.

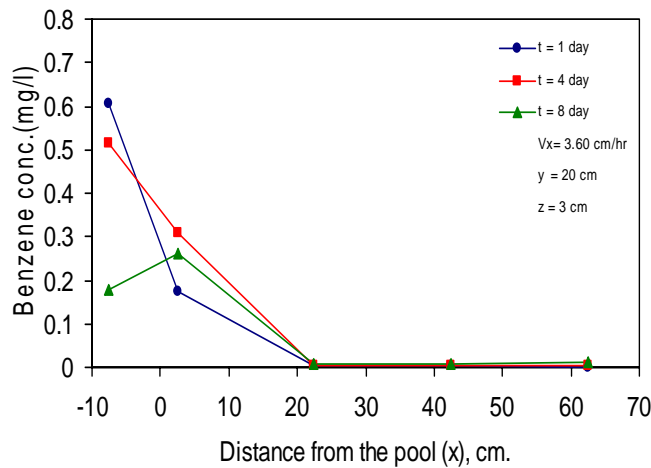
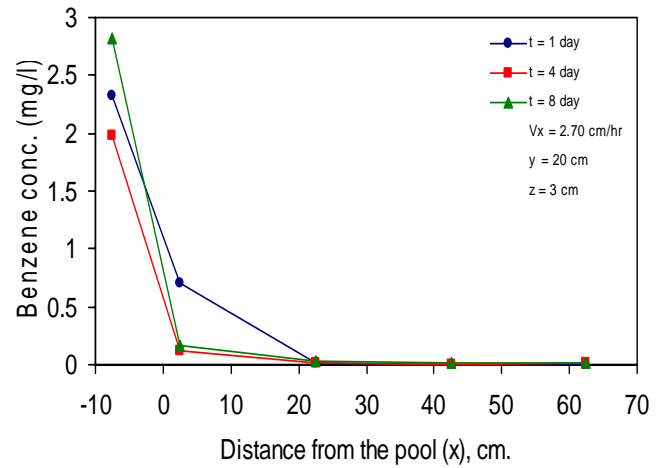
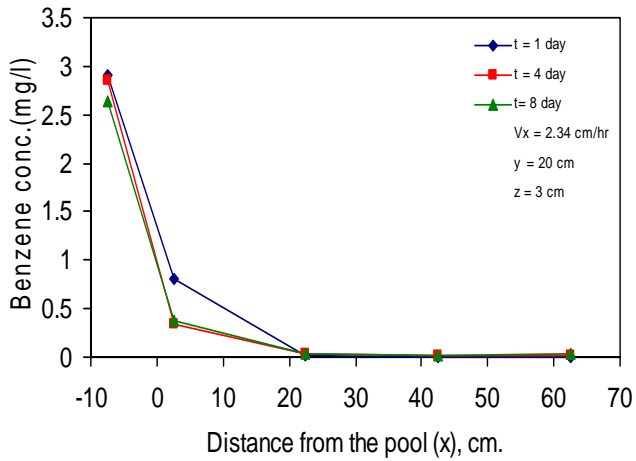
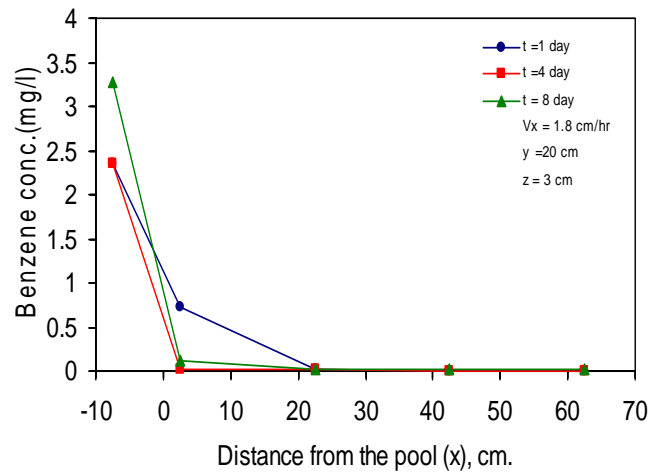
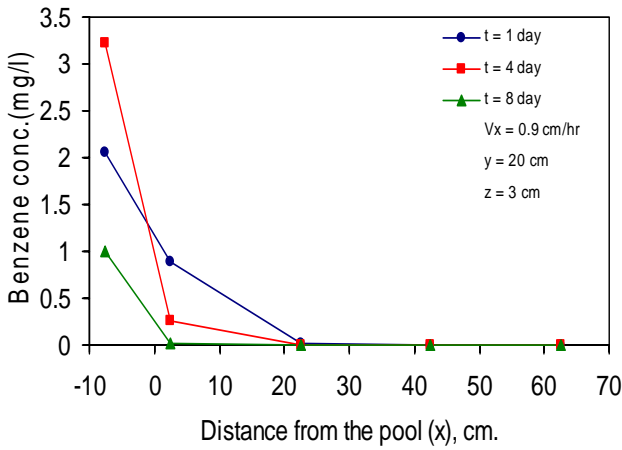


Figure 5: The measured concentration of benzene versus distance from the pool (x) at interstitial velocity 0.90, 1.80, 2.34, 2.70, and 3.60 cm/hr, cm/hr, depth (z) 3 cm, $y = 20$ cm, and times 1, 4, 8 day.

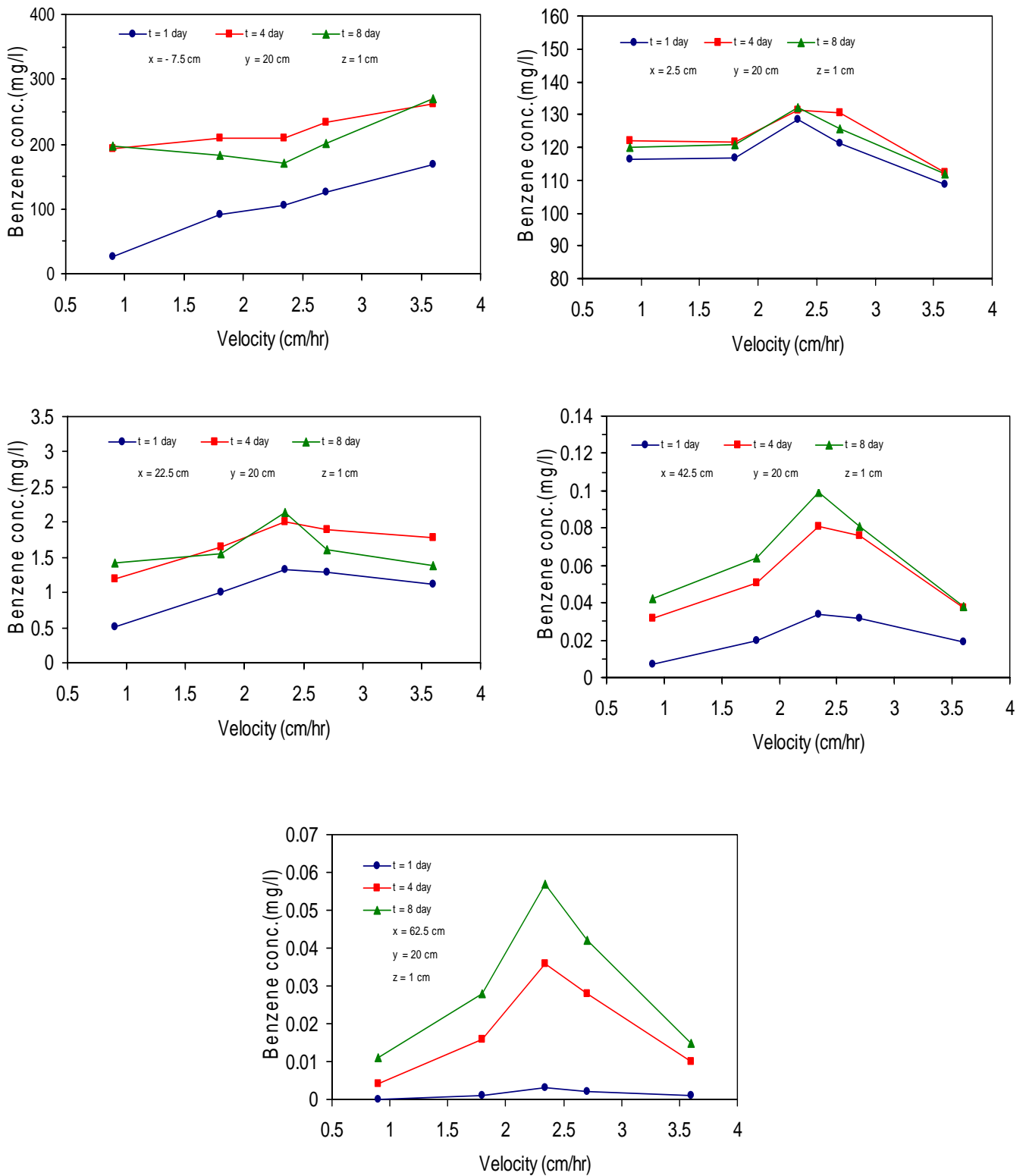


Figure 6: The measured concentration of benzene versus the interstitial velocity (V_x) at depth (z) 1 cm, The distance from the pool (x) - 7.5, 2.5, 22.5, 42.5, and 62.5 cm, $y = 20$ cm, and times 1, 4, 8 day.

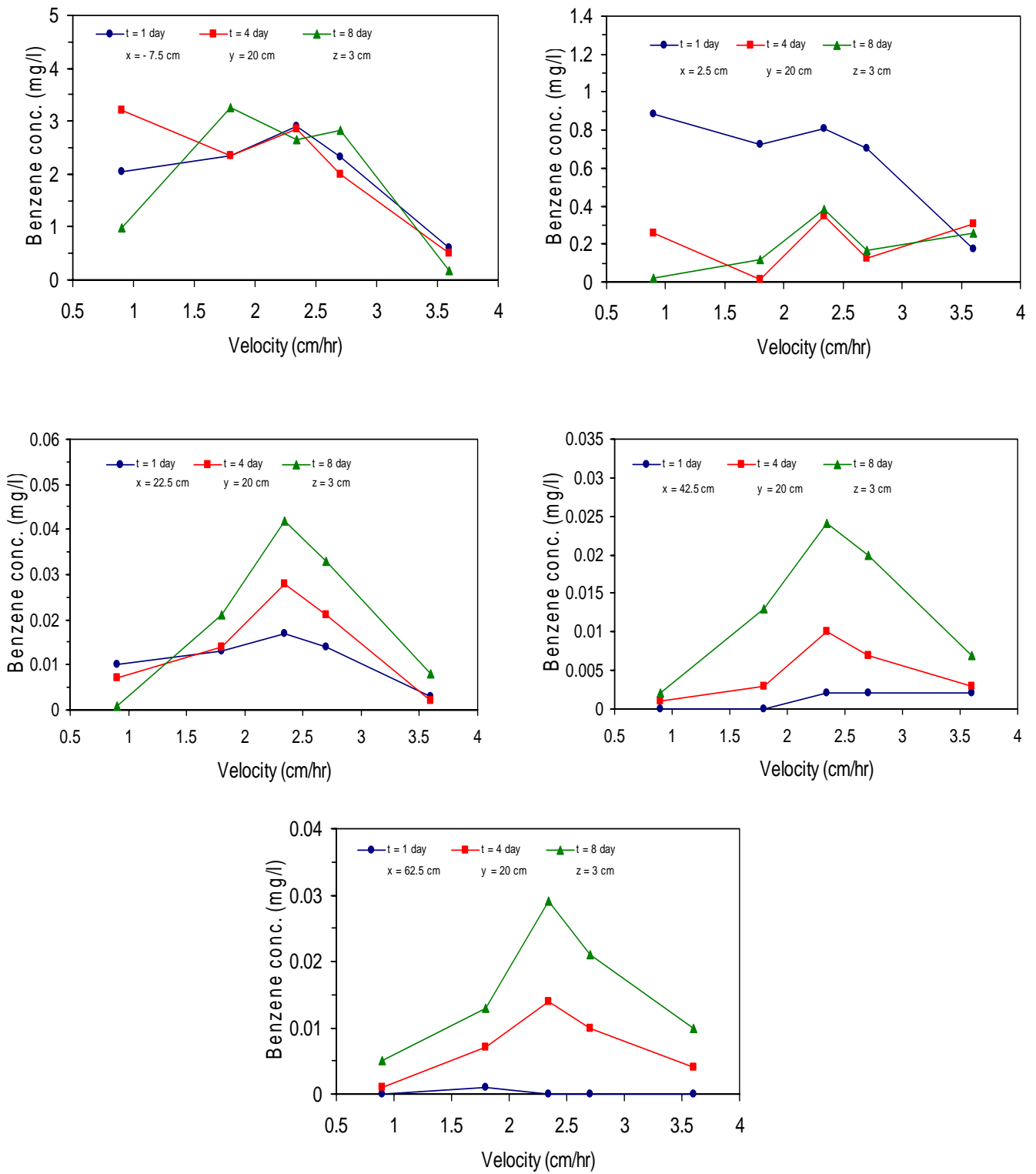


Figure 7: The measured concentration of benzene versus the interstitial velocity (V_x) at depth (z) 3 cm, distance from the pool (x) -7.5 cm, 2.5, 22.5, 42.5, and 62.5 cm, $y = 20$ cm, and times 1, 4, 8 day.

4. MASS TRANSFER CORRELATION:

Power and Heermann (1999) reported that the average mass-transfer coefficient (k^*) can be computed from the following equation:

$$k^* = n \sqrt{\frac{4D_z V_x}{\pi L}} \quad (2)$$

where L is the length of interface.

Time invariant, average mass transfer correlations for NAPL pool dissolution in saturated porous media were developed by Kim and Chrysikopoulos (1999), based on numerically determined average mass transfer coefficients

evaluated for interstitial fluid velocities of 0.3, 0.5, 0.7, and 1.0 m/day.

The time invariant average mass transfer coefficient (k^*) was experimentally determined using equation (2) for each velocity. The vertical dispersion coefficient (D_z) is 2.84×10^{-2} , 5.53×10^{-2} , 6.96×10^{-2} , 7.80×10^{-2} , and 1.014×10^{-1} cm²/hr at the velocities 0.90, 1.80, 2.34, 2.70, 3.60 cm/hr respectively (Gzar, 2010). Figure (8) indicates that k^* is proportional to the interstitial velocity (V_x). This behavior is attributed to increasing the concentration gradients at the NAPL-water interface with increasing V_x . The best fit relation of the time invariant average mass transfer coefficient (k^*) as a function to interstitial velocity (V_x) is:

$$k^* = 0.0166 V_x + 0.0016 \quad (3)$$

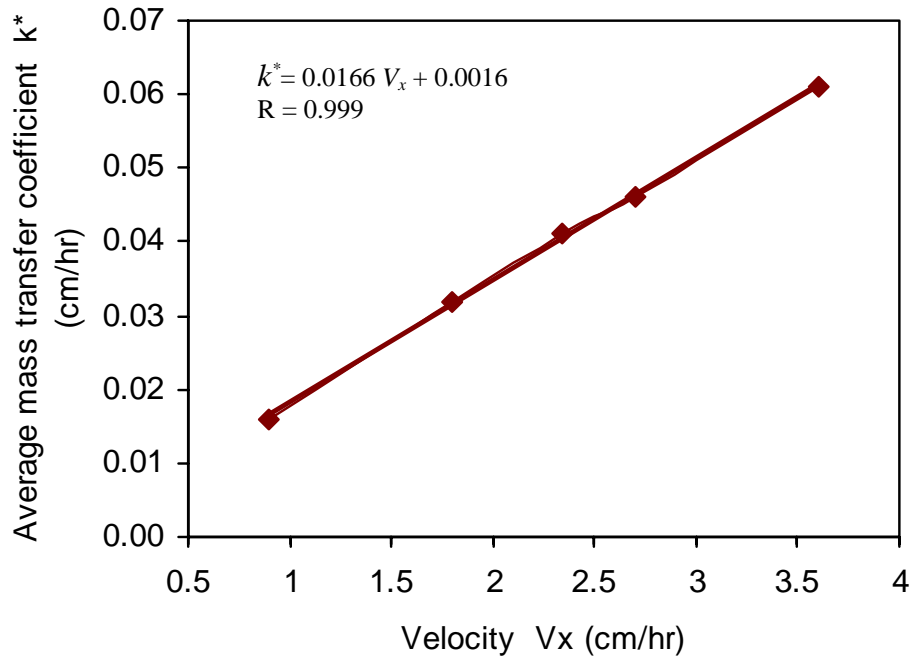


Figure 8: The change of the average mass transfer coefficient (k^*) with the interstitial velocity (V_x).

The dimensionless mass transfer behavior is summarized in terms of the modified Sherwood number, $Sh^*_{(e)} = k^* l_{c(e)}/D_e$, (figure 9), where the characteristic length ($l_{c(e)}$) employed here is the square root of the pool area. The computed $l_{c(e)}$, and D_e for the present research were 13.29 cm and $2.47 \cdot 10^{-2}$ cm²/hr respectively.

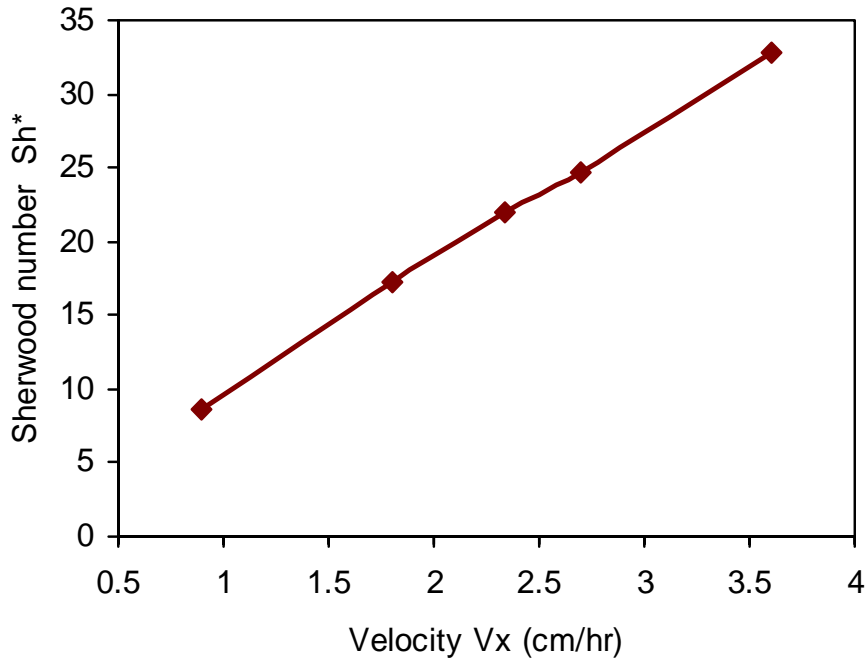


Figure 9: The dimensionless mass transfer (modified Sherwood number $Sh^*_{(e)}$) behavior with the interstitial velocity (V_x).

5. CONCLUSIONS:

A three dimensional bench-scale aquifer has been designed and constructed for dissolution experiments. The concentration profile with time is determined at different distances near the water table at different values of the interstitial velocity. A relationship is found between the time invariant average mass transfer coefficient and the interstitial velocity. The values of this coefficient are ranged from 0.016 to 0.061 cm/hr. It is increased proportionally with velocity toward a limiting value. The results show that the concentration of the LNAPL reduces as the distance increased in x and/or z direction from the source of pollution. In most cases the concentration declines with velocity more than 2.34

cm/hr at distances downstream of the LNAPL pool.

References:

- Al-Khafaji A.W., and Andersland O.B., "Geotechnical engineering and soil testing", Saunders College Publishing, 1992.
- Bowles J.E., " Engineering properties of soils and their measurement ", McGraw-Hill Kogakusha, Ltd., 1978.
- Christensen, J.S., and J. Elton, "Soil and ground-water pollution from BTEX". www.cee.vt.edu/program_areas/environmental/teach/gwprimer/btex/btex.html, 2005.
- Chrysikopoulos C.V., and Kim T-J, "Local mass transfer correlations for nonaqueous

phase liquid pool dissolution in saturated porous media", *Transp. Porous Media*, 38, 167-187, 2000.

Clement T.P. , Kim Y.C., Gautam T.R., and Lee K.K. "Experimental and numerical investigation of DNAPL dissolution process in a laboratory aquifer model", *Journal of Ground water Monitoring & Remediation* , 24(4), 88-96, 2004.

Gzar H. A., "Experimental investigation and numerical modeling of benzene dissolution and transport in a saturated zone of the soil", Ph.D. thesis, College of Engineering/ University of Baghdad, 2010.

Hiscock K., " Ground-water pollution and protection", Environmental Science for Environmental Management, O'Riordan (eds),1995.

Kim T-J, and Chrysikopoulos C.V., "Mass transfer correlations for nonaqueous phase liquid pool dissolution in saturated porous media", *Water Resour. Res.* , 35 449-459, 1999.

Lee K.Y. and Chrysikopoulos C.V., "Dissolution of a multicomponent DNAPL pool in an experimental aquifer", *Journal of Hazardous Materials*, B128, 218-226, 2006.

Mackay D.M., Roberts P.V., Cherry J.A., "Transport of organic contaminants in ground-water: distribution and fate of chemicals in sand and gravel aquifers", *Environ. Sci. Technol.*, 19 (5), 384-392, 1985.

Makri P., Kalivas D.K., Bathrellos G., and Skilodimou H., "Spatio-temporal analysis of ground-water pollution from BTEX in Thriassio Field, Attica, Greece", *IAEG*, paper number 409, 2006.

Moore G.S., Villenave J.H., and Hickey J.C., "Characterization of petroleum contaminants in ground-water and soils", Hydrocarbon contaminated soil In:

Kostecki P., Calabrese E., and Bonazountas M. (eds).Chelsea Lewis Publishers, USA, 1992.

Newell C.J., Acree S.D., Ross R.R., and Huling S.G., "Light nonaqueous phase liquids", EPA Ground Water Issue, EPA/540/S-95/500, September 1995.

Phophi T.S., "The occurrence and evaluation of LNAPLs contamination in urban areas of South Africa", Master thesis, University of the Free State, Bloemfontein, South Africa, 2004.

Power S.E. and Heermann S.E., " Potential ground and surface water impacts, appendix B: Modeling interface mass-transfer processes" presented in "A critical review: the effect of ethanol in gasoline on the fate and transport of BTEX in the subsurface", Editors Cannon G. and Rice D. , UCRL-AR-135949 Vol.4, chapter 2, 1999.